Physica B: Condensed Matter 534 (2018) 76–82

Contents lists available at ScienceDirect

Physica B: Condensed Matter

journal homepage: www.elsevier.com/locate/physb

Effect of doping rare earths on magnetostriction characteristics of $CoFe_2O_4$ prepared from spent Li-ion batteries

Guoxi Xi *, Tingting Zhao, Lu Wang, Changwei Dun, Ye Zhang

Key Laboratory for Yellow River and Huai River Water Environment and Pollution Control, Ministry of Education, College of Chemistry and Chemical Engineering, Henan Normal University, Xinxiang, 453007, PR China

ARTICLE INFO

Keywords:
Spent Li-ion batteries
Rare earth
Cobalt ferrite
Magnetic materials
Magnetostriction

ABSTRACT

Recovering spent Li-ion batteries is beneficial to the economy and environment. Therefore, this study synthesized nanoparticles of cobalt ferrite doped with different rare earth ions (Nd, Ce, and Pr) by a sol-gel auto-combustion method using spent Li-ion batteries. The effect of the different doping elements on grain sizes, structure, magnetic and magnetostrictive properties, and strain derivative were confirmed by X-ray diffraction, scanning election microscopy, vibrating sample magnetometer, and a magnetostrictive coefficient measuring system. Substitution of a small amount of Fe^{3+} with RE^{3+} in $CoRE_xFe_{2-x}O_4$ ($x = 0.025$, 0.05, and 0.1) had a large effect on magnetostrictive properties and strain derivative, which was improved compared with pure cobalt ferrite at low magnetic field. The maximum strain derivative ($d\lambda/dH = -1.49 \times 10^{-9}\ A^{-1}\ m$ at 18 kA m^{-1}) was obtained for Nd, $x = 0.05$. Changes in the magnetostriction coefficients and strain derivatives were correlated with changes in cation distribution, microstructure, and magnetic anisotropy, which depended strongly on RE^{3+} substitution and distribution in the spinel structure.

1. Introduction

Li-ion batteries have become very popular energy sources for mobile applications, such as cell phones, hybrid and electric vehicle, etc., and the demand will increase further with ongoing development of the hybrid electric vehicle industry. Rapid development of Li-ion batteries has brought convenience to people's life, but they have only 2–3 years life, which has led to increasing battery scrap generation, which must be recycled for sustainable development of the economy and environment. Li-ion batteries contain a lot of valuable metal resources, such as cobalt, iron, copper, and nickel, which means spent Li-ion batteries have significant residual value. Therefore, many studies have considered recycling spent Li-ion batteries [1–7].

Magnetostriction materials have been intensively studied and reported since they were discovered. Joule found that magnetostrictive materials can transform energy between magnetic and elastic states in 1842. The alloy based magnetostrictive smart material Terfenol-D has been applied in many fields, such as ultrasonic generation, stress sensing, and vibration control. Recently, cobalt ferrite ($CoFe_2O_4$) has been widely studied to overcome some alloy material drawbacks of high cost, poor mechanical properties, and low magnetocrystalline anisotropy [8,9]. Therefore, using spent Li-ion batteries to prepare cobalt ferrite not only provides cost-effective and easily accessible raw materials, but also alleviates resource shortage.

Crystalline cobalt ferrite is $(Co_x^{2+}Fe_{1-x}^{3+})[Co_{1-x}^{2+}Fe_{1+x}^{3+}]O_4$, where x is the fraction of tetrahedral sites (A-sites) occupied by Co^{2+} ions. Thus, crystalline $CoFe_2O_4$ has a mixed spinel structure, related to preparation conditions and heat treatment procedures [9–11]. The Co^{2+} ions tend to occupy octahedral sites (B-sites) and the concentration at the B-sites has a strong influence on $CoFe_2O_4$ performance. Therefore, changing the cation distribution by substituting Co^{2+} or Fe^{3+} with different metal ions, such as Mn, Ca, Al and Ni, will influence cobalt ferrite magnetic and magnetostrictive properties, which have been widely studied [12–15].

The magnetostriction strain coefficient (λ) and strain sensitivity ($d\lambda/dH$) under an applied magnetic field are important factors for cobalt ferrite applications, and enhancing their values is a significant research direction for many applications. Introducing a small amount of rare earth (RE) ions into the spinel lattice to modify the structure and improve magnetostrictive properties of cobalt ferrite has attracted much attention. The 4f electron shells (from 0 (La) to 14 (Lu)) and magnetic moments (from 0 (La) to 10.6 μ_B (Dy)) of the RE ions have spin-orbit coupling to the angular momentum. Doping RE ions into the spinel cobalt ferrites can cause 3d-4f coupling, which determines large magnetocrystalline anisotropy and magnetic behavior. Substituting RE

* Corresponding author.
E-mail addresses: hnsdxgx@163.com (G. Xi), hnsdztt@163.com (T. Zhao).

https://doi.org/10.1016/j.physb.2018.01.036
Received 19 September 2017; Received in revised form 15 January 2018; Accepted 16 January 2018

elements with large ionic radii for the smaller ionic radii Fe^{3+} within $CoFe_2O_4$ can modify cell parameters, average crystallinity, and grain, which will modify magnetic and magnetostrictive properties [16,17].

Previous studies have synthesized cobalt ferrite with spent Li-ion batteries using the sol-gel hydrothermal method and different metal ions substitution for Co^{2+} or Fe^{3+} using sol-gel auto-combustion [18–20]. However, magnetostrictive properties and strain derivative require further improvement for practical applications. The current study used three different Lanthanide ions with different ionic radii and magnetic moments to modify cobalt ferrite, and compared and contrasted the influence of the RE elements on the final assembly properties. Significant improvement in strain sensitivity was achieved at low doping levels in sintered RE doped cobalt ferrites.

2. Experimental details

A series of RE doped cobalt ferrite samples, $CoRE_xFe_{2-x}O_4$ (RE = Ce, Pr and Nd; x = 0.025, 0.05 and 0.1) were obtained by sol-gel auto-combustion using spent Li-ion batteries collected from mobile phones for raw materials. Cathode materials ($LiCoO_2$) were separated from the spent batteries and dissolved in nitric acid solution containing a small amount of hydrogen peroxide. Precipitations containing Co^{2+} and Fe^{3+} were generated by adjusting the pH with ammonia, then filtered and re-dissolved in nitric acid to obtain the mixed solution [21]. $Co(NO_3)_2{\cdot}6H_2O$, $Fe(NO_3)_3{\cdot}9H_2O$ and $RE(NO_3)_3{\cdot}6H_2O$ were added to the mixed solution to adjust Co^{2+}, Fe^{3+}, and RE^{3+} ion concentrations, respectively, in accordance with the stoichiometry. Citric acid was added to the mixed solution at a 1:1 ratio of metal ion concentration to citric acid and the mixture was constantly stirred at 60 °C until completely dissolved. The final solution pH was adjusted to 6.5 using ammonia at the same temperature to obtain a solution, which was then heated to 80 °C, stirred using a magnetic stirrer to form a gel, and transferred to an air dry oven at 100 °C for 48 h. Approximately 2 mL alcohol was added to the dried sample and ignited, until it was completely burnt to ashes, then ground into power. Full details of the method are available in our previous literature [18,20].

X-ray diffraction (XRD, D8-advance, BRUKER, Karlsruhe, Germany) with monochromatic graphite showed that these samples had characteristics consistent with cobalt ferrite. Microstructures of the sintered samples were obtained by field emission scanning electron microscopy (FESEM, SUPRA-40, Carl Zeiss, Jena, Germany). Then the samples were mixed with 8%–10% polyvinyl alcohol (PVA) and pressed into the desired shape: cylindrical, 10 × 20 mm diameter × length using a uniaxial hydraulic press at 12 MPa. The pressed compacts were sintered at 1450 °C for 6 h with heating/cooling rate 5 °C/min. The magnetostrictive properties of final pure and doped cobalt ferrite samples were investigated by a JDM-30 magnetostrictive coefficient measuring system.

3. Results and discussions

Fig. 1a–c shows X-ray diffraction patterns for pure and doped cobalt ferrite with different RE contents. These were characterized at room temperature with sweep speed interval 0.02° and 20°–80° (2θ) angular extension. The diffraction peaks are sharp and correspond to a cubic spinel ferrite structure (JCPDS, No. 22-1086). Impurity peaks (marked "*" in Fig. 1) were observed in Pr and Nd doped cobalt ferrite ($REFeO_3$) and Ce doped cobalt ferrite (CeO_2) (JCPDS, No. 34-0394). The orthoferrite phase was not observed for Ce doped cobalt ferrite, which may be due to the higher CeO_2 refractory temperature. These effects were consistent with previous studies [17,22,23]. Impurity peaks were considered to be RE^{3+} partial replacement of Fe^{3+} into the spinel lattice, due to limited solubility, which caused excess RE^{3+} ions to accumulate on the grain boundaries and form a secondary phase. Average $CoRE_xFe_{2-x}O_4$ particle size (d_{XRD}) was calculated from full width at half maximum (FWHM) of the XRD peaks with maximum intensity using Scherrer's formula, as shown in Table 1,

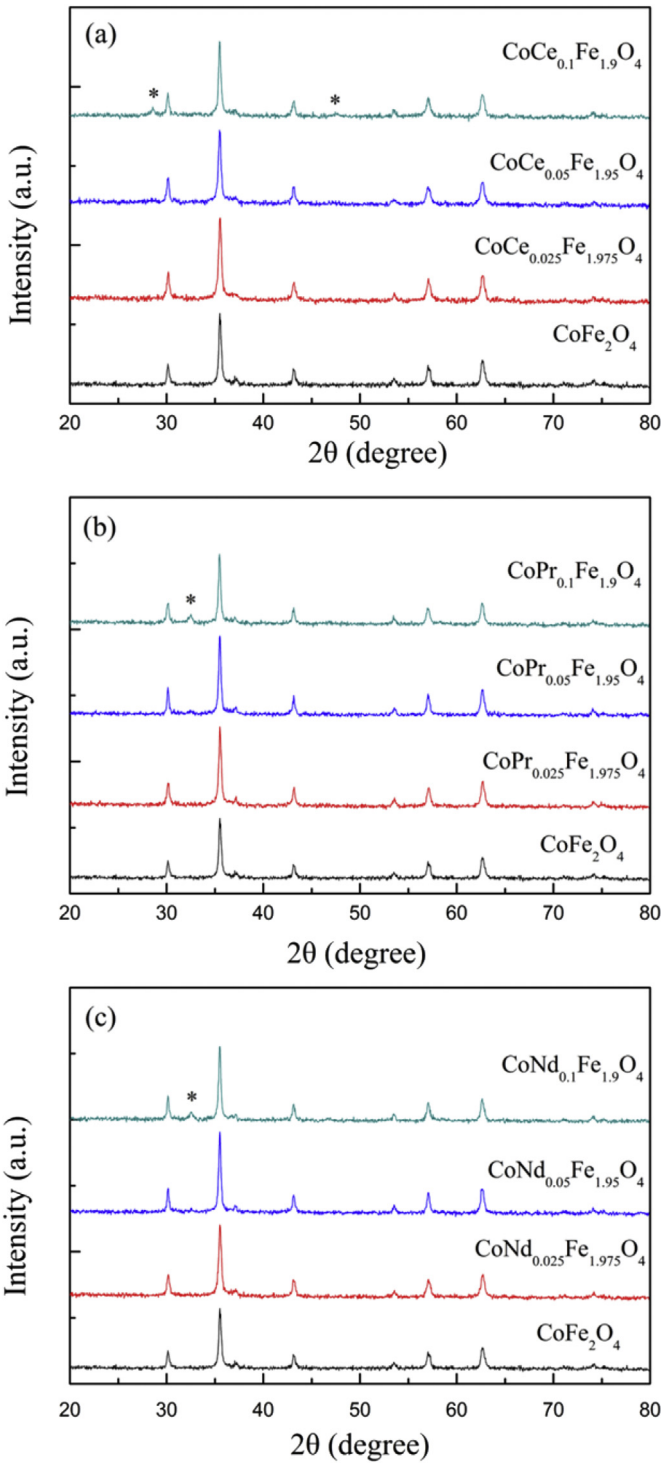

Fig. 1. XRD patterns for (a) $CoCe_xFe_{2-x}O_4$, (b) $CoPr_xFe_{2-x}O_4$ and (c) $CoNd_xFe_{2-x}O_4$ (x = 0.025, 0.05, and 0.1).

$$d_{XRD} = k\lambda/\beta \cos\theta \quad (1)$$

where d_{XRD} is the average crystallite size; k = 0.9 is the Scherrer constant; λ = 1.5406 Å is the radiation wavelength; β is the half width of the relevant diffraction peak; and θ is the Bragg angle.

The lattice parameter, a, for $CoRE_xFe_{2-x}O_4$ can be expressed as

$$a = \lambda\left(h^2 + k^2 + l^2\right)^{1/2} \Big/ 2\sin\theta \quad (2)$$

Table 1
Average crystallite size and lattice parameters of $CoFe_2O_4$, $CoCe_xFe_{2-x}O_4$, $CoPr_xFe_{2-x}O_4$ and $CoNd_xFe_{2-x}O_4$.

Sample	x	d_{XRD} (nm)	a (Å)
$CoFe_2O_4$	0.00	27.08	8.377
$CoCe_xFe_{2-x}O_4$	0.025	25.13	8.369
	0.05	26.40	8.385
	0.1	28.76	8.386
$CoPr_xFe_{2-x}O_4$	0.025	28.47	8.378
	0.05	29.47	8.378
	0.1	29.89	8.386
$CoNd_xFe_{2-x}O_4$	0.025	25.41	8.377
	0.05	30.44	8.378
	0.1	29.06	8.378

where (h k l) is the most intense peak (311). Compared with pure cobalt ferrite, small amounts of RE^{3+} (Ce^{3+} and Nd^{3+}, x = 0.025) substituting for Fe^{3+} decreases the average particle size and lattice constant (Table 1), which is consistent with Bulai et al. [17]. Changes of average particle sizes and lattice parameters had a positive correlation with RE^{3+} concentration at $CoRE_xFe_{2-x}O_4$ (x = 0.025 to 0.1). However, average particle size was maximum d_{XRD} = 30.44 nm for $CoNd_xFe_{2-x}O_4$ (x = 0.05). Changes of average particle and lattice parameters can be attributed to lattice strain caused by replacement of smaller Fe^{3+} (0.64 Å) ions by larger RE^{3+} (Ce^{3+} (1.034 Å), Pr^{3+} (1.01 Å), and Nd^{3+} (0.995 Å)) ions in the spinel ferrite lattice.

Fig. 2a–d shows example FESEM micrographs, which were used to investigate the structure of pure and RE doped cobalt ferrite ($CoRE_{0.025}Fe_{1.975}O_4$ example). Samples prepared by sol-gel auto-combustion had a thicker thin sheet formed by aggregation of small particles, and porous morphology, which was attributed to the amount of gases that escape during combustion [18]. Pure cobalt ferrite had smaller grains in comparison with RE doped samples and the average grain sizes decreased from Fig. 2b–d, which may be because the RE^{3+} ion size decreased from Ce^{3+} to Nd^{3+}. Grain sizes of $CoCe_{0.025}Fe_{1.975}O_4$ (Fig. 2b) were larger than the other cases, which may be ascribed to the larger ionic radius and formation of a CeO_2 phase that accumulated at grain boundaries [17]. Thus, morphology and structure changes of the cobalt ferrites were influenced by the different RE^{3+} ions and solubility limits [18].

Hysteresis loops were measured at room temperature to characterize the magnetic properties of $CoRE_xFe_{2-x}O_4$ samples sintered at 1450 °C, as shown in Fig. 3a–c. Table 2 shows the saturation magnetization, M_s. Small amounts of RE^{3+} can change M_s of cobalt ferrite and the M_s for each RE-doped sample can be divided as follows. (1) Ce^{3+} and Pr^{3+} doped samples cause increased M_s at $CoRE_xFe_{2-x}O_4$ (x = 0.025), then decrease at x = 0.05; (2) M_s in Nd doped samples decreased with increasing concentration compared with pure cobalt ferrite at x = 0.025–0.05; (3) M_s showed no significant change from x = 0.05–0.1 for RE doped samples.

These results may be influenced by multiple factors. (a) Super-exchange between A-site and B-site cations, RE^{3+} substitution for Fe^{3+} in the spinel lattice contribute to migration of Co^{2+} ions from the B-sites to the A-sites [24,25]. Trace amounts of RE^{3+} in the lattice can cause RE^{3+}-Fe^{3+} (3d-4f coupling) and RE^{3+}-RE^{3+} (4f-5d-4f coupling) interactions. (b) The second orthoferrite phase was formed with increasing concentration, and accumulated on the grain boundaries, blocking the magnetic response of the samples; (c) The effective magnetic moment of RE^{3+} ions are less than Fe^{3+} ions, which may be the reason for decreased M_s. Variations in coercivity, H_c, are shown in Fig. 3a–c insets, and correlated with the microstructure and anisotropy constant,

$$H_c = 2K_1/\mu_0 M_s \quad (3)$$

where μ_0 is the initial permeability; and K_1 is the magnetostriction

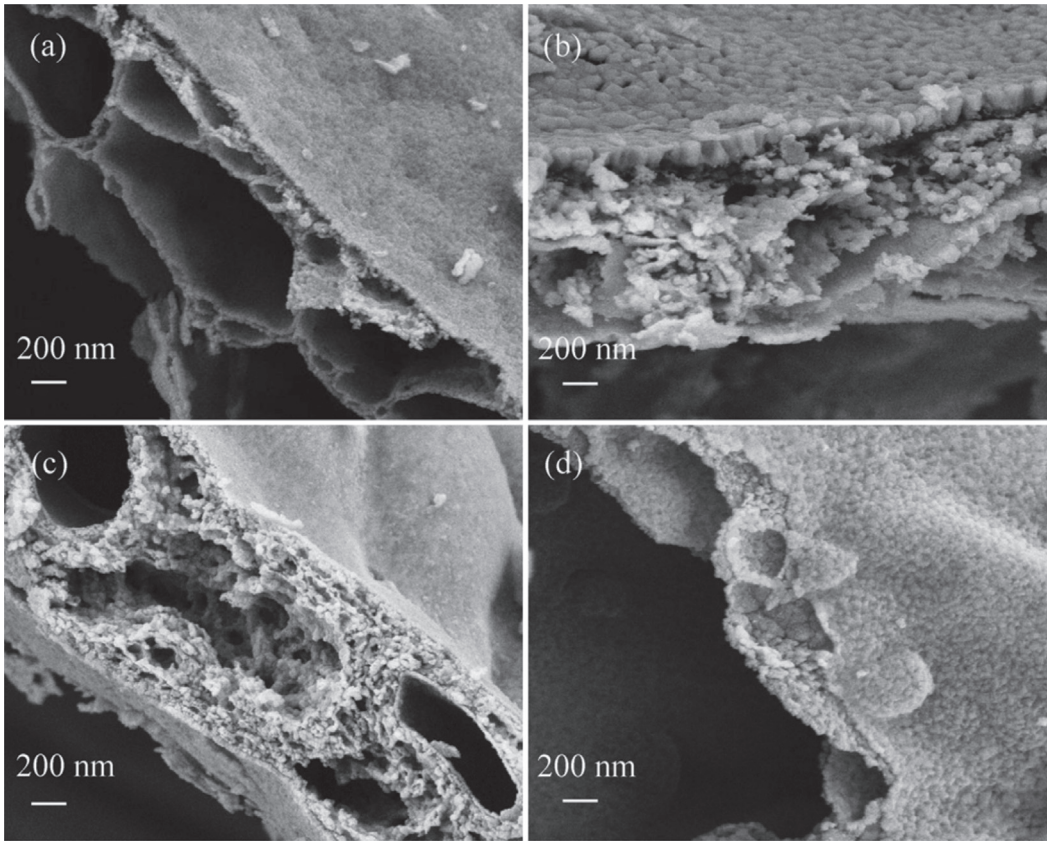

Fig. 2. FESEM images for (a) $CoFe_2O_4$, (b) $CoCe_{0.025}Fe_{1.975}O_4$, (c) $CoPr_{0.025}Fe_{1.975}O_4$, (d) $CoNd_{0.025}Fe_{1.975}O_4$.

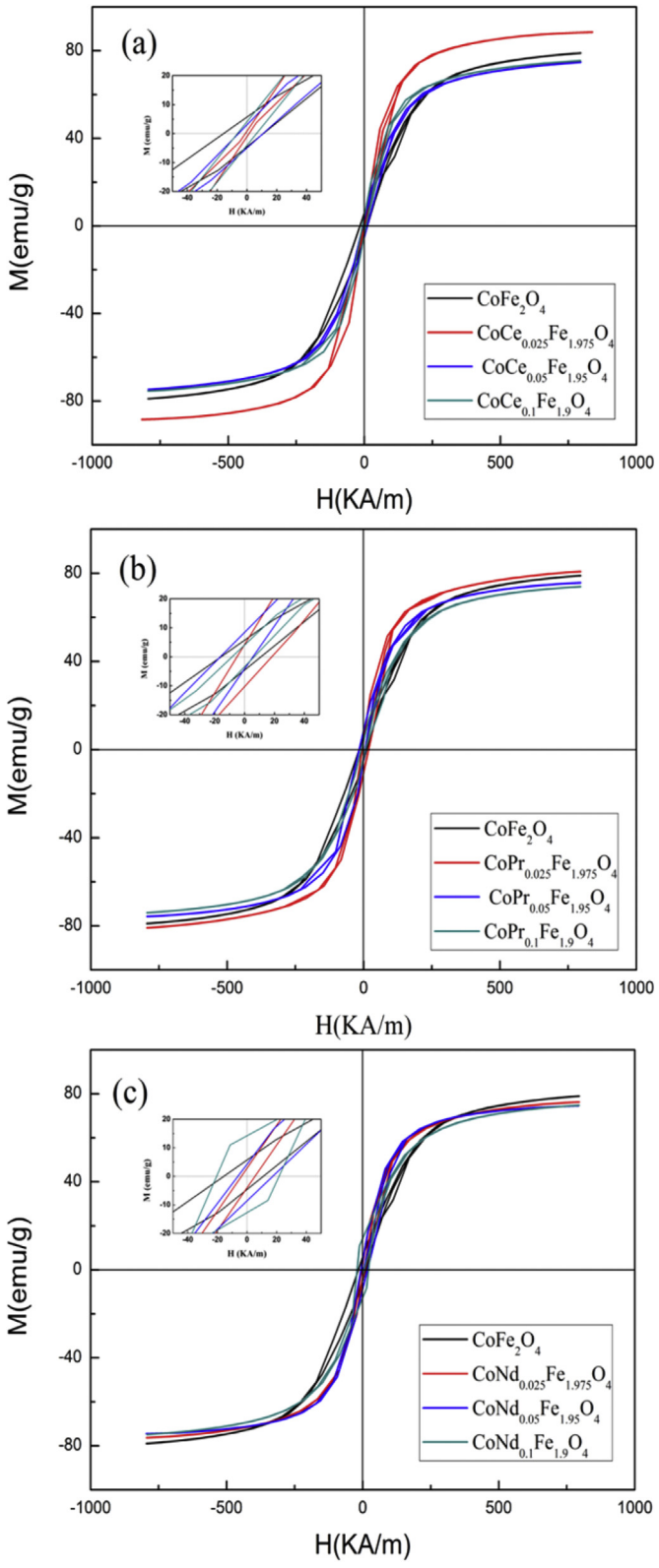

Fig. 3. Magnetic hysteresis of sintered (a) $CoCe_xFe_{2-x}O_4$, (b) $CoCe_xFe_{2-x}O_4$ and (c) $CoCe_xFe_{2-x}O_4$ (x = 0.025, 0.05, and 0.1) at room temperature.

anisotropy coefficient, which exhibits a similar trend to H_c. The microstructures of the sintered samples are different, which may be the underlying reason for the coercivity disparity.

Fig. 4a–c shows magnetostrictive and strain derivative curves for the sintered samples, measured at room temperature, and Table 2 shows the

Table 2
Magnetic and magnetostriction parameters of $CoFe_2O_4$, $CoCe_xFe_{2-x}O_4$, $CoPr_xFe_{2-x}O_4$, and $CoNd_xFe_{2-x}O_4$.

Sample	x	M_s (emu/g)	λ_{max} (ppm)	Field at λ_{max} (kA m^{-1})	$(d\lambda/dH)_{max}$ (10^{-9} A^{-1} m)	Field at $(d\lambda/dH)_{max}$ (kA m^{-1})
$CoFe_2O_4$	0.00	78.96	−180.7	399	−1.18	93
$CoCe_xFe_{2-x}O_4$	0.025	88.49	−121.6	256	−1.05	37
	0.05	74.69	−134.6	263	−1.19	66
	0.1	75.44	−116.9	225	−1.46	38
$CoPr_xFe_{2-x}O_4$	0.025	80.84	−140.5	251	−1.29	38
	0.05	75.72	−127.0	216	−1.33	32
	0.1	73.99	−126.7	318	−0.86	52
$CoNd_xFe_{2-x}O_4$	0.025	76.28	−152.5	275	−1.20	53
	0.05	74.53	−131.0	244	−1.49	18
	0.1	74.88	−111.6	295	−0.77	46

M_s: saturation magnetization; λ_{max}: maximum magnetostriction strain; Field at λ_{max}: field at maximum magnetostriction strain; Field at $(d\lambda/dH)_{max}$: field at maximum strain sensitivity.

maximum magnetostrictive coefficient (λ_{max}), maximum strain derivative ($(d\lambda/dH)_{max}$), and corresponding field at λ_{max} and ($(d\lambda/dH)_{max}$). Sintered samples showed maximum λ_{max} for pure cobalt ferrite, RE doping decreased λ_{max} with increasing ion concentration. Pure cobalt ferrite had a $\lambda_{max} = -180.7$ ppm at 399 kA m^{-1}, whereas RE doped cobalt ferrite had maximum $\lambda_{max} = -152.5$ ppm at 275 kA m^{-1}, for $CoNd_{0.025}Fe_{1.975}O_4$. The λ_{max} for RE doped cobalt ferrite decreased with increasing RE^{3+} concentration except Ce^{3+}, which had a λ_{max} at x = 0.05. Importantly, all λ_{max} values of RE doped samples were obtained at lower magnetic field than pure cobalt ferrite.

The variation due to $CoRE_xFe_{2-x}O_4$ doping can be explained as follows. Co^{2+} and Fe^{3+} ions in the octahedral site of the spinel crystal structure have larger influence on magnetostriction compared with cations at tetrahedral sites [26,27]. RE^{3+} replacement for Fe^{3+} tend to occupy B-sites, hence RE^{3+} ions distorted the spinel crystal structure, changing the magnetostrictive state [17]. RE^{3+} substitution and sintering processes increase grain size and lattice parameter variation, contributing to magnetostrictive strain [26]. High magnetostriction at low magnetic fields for the RE doped materials may be exploited for sensors and actuators, e.g. stress and torque sensing, etc. [28].

Fig. 4a–c shows the strain derivative, dλ/dH, for the applied magnetic field for different RE doped cobalt ferrites. The strain derivatives were influenced by RE doping, but were not linear with dope rate, in contrast to previous studies [18]. The current study shows that Nd and Pr doped cobalt ferrite had larger $(d\lambda/dH)_{max}$ than pure cobalt ferrite for $x \leq 0.05$, then decreased below pure cobalt ferrite. The $(d\lambda/dH)_{max}$ for the Ce doped cobalt ferrite was lower than pure cobalt ferrite for $x \leq 0.025$, then increased with increasing concentration. Maximum strain derivative variations for RE doped cobalt ferrites were obtained at a lower magnetic field than pure cobalt ferrite. This may be due to different secondary phases on the grain boundary for the RE doped cobalt ferrites producing lattice and magnetocrystalline anisotropy. Strain derivation can be expressed as [28].

$$dB/d\sigma = d\lambda/dH = 2\mu_0\lambda_s M/NK_1 \quad (4)$$

where $dB/d\sigma$ is the sensitivity of the magnetization to stress or torque, M is the magnetization, λ_s is the saturation magnetostriction and N is a constant depending upon the anisotropy of the materials.

The ratio of saturation magnetostriction to magnetostriction anisotropic coefficient, λ_s/K_1, is an important factor in determining the strain sensitivity, and λ_s is strongly related to the position of the ions in the cubic spinel ferrite structure. Co^{2+} ions in B-sites can create stronger anisotropy than in A-sites [26]. Co^{2+} from the B-sites transfer to the A-sites in the cubic spinel ferrite structure, because the RE^{3+} ions replace the Fe^{3+} and occupy the B-sites, which may decrease K_1, increase λ_s/K_1, and increase strain sensitivity. Another factor affecting strain sensitivity may relate to the sintering process and microstructure. All the samples

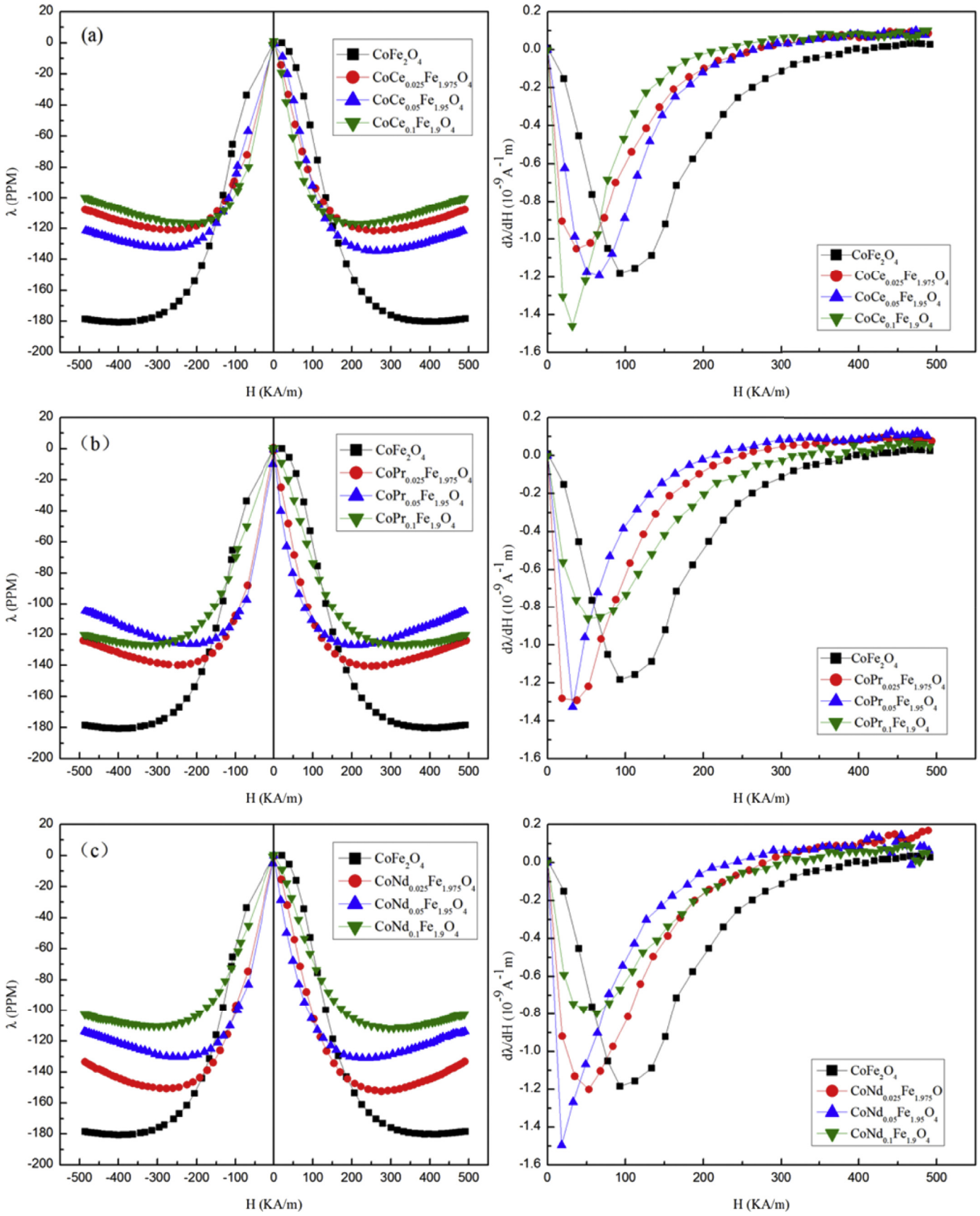

Fig. 4. Magnetostrictive and derivative curves for sintered (a) $CoCe_xFe_{2-x}O_4$, (b) $CoCe_xFe_{2-x}O_4$, and (c) $CoCe_xFe_{2-x}O_4$ (x = 0.025, 0.05, and 0.1).

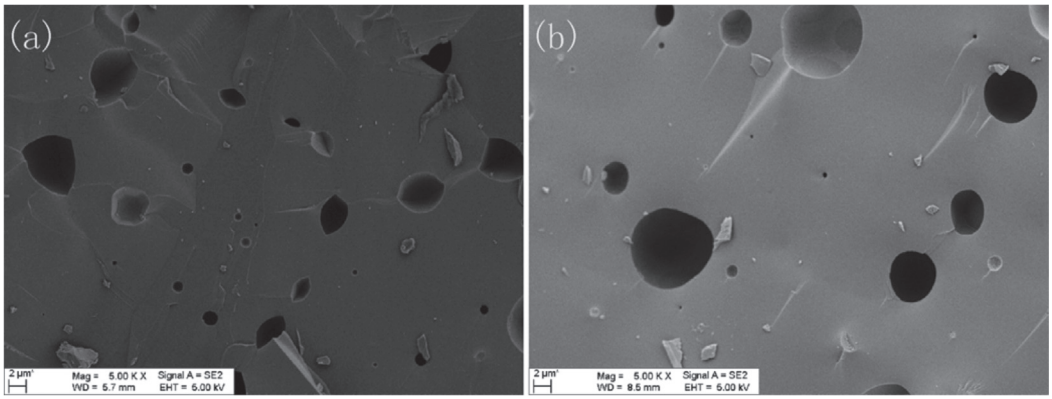

Fig. 5. FESEM images for (a) $CoFe_2O_4$ and (b) $CoNd_{0.025}Fe_{1.975}O_4$ after sintering at 1450 °C for 6 h.

were synthesized under the same conditions, therefore, the change of λ_s may be due to microstructure changes caused by different concentrations of RE^{3+} substitution Fe^{3+} in the spinel cobalt ferrite.

Fig. 5a and b shows FESEM images for $CoFe_2O_4$ and $CoNd_{0.025}Fe_{1.975}O_4$ sintered samples at 1450 °C. Significant changes in the microstructure are evident, compared with powder samples before sintering. Disappearance of the grain was attributed to high temperature continuous sintering contributing to increased grain size, and the images show many large intragranular pores due to gases released from the spinel lattice and high PVA content in the process, which may be another reason for the lower magnetostriction, as reported in the literature [9, 29].

4. Conclusions

Magnetostriction was studied for different RE doped cobalt ferrite samples derived from nanocrystalline powders prepared by a sol-gel auto-combustion route using spent Li-ion batteries. Incorporation of RE^{3+} in the spinel lattice modified the cobalt ferrite microstructure, and significant improved magnetostriction characteristics at lower magnetic field strength.

The best magnetostriction (−152.5 ppm) were obtained for $CoNd_xFe_{2-x}O_4$ at 276 kA m^{-1} for x = 0.025, whereas the maximum strain derivative was -1.49×10^{-9} A^{-1} m, at 18 kA m^{-1} for x = 0.05. Rare earth doped cobalt ferrites did not enhance magnetostriction coefficient, and even decreased for higher RE concentration. However, the maximum magnetostrictive characteristics obtained recommend such materials for applications in the automotive sensors field. Therefore, RE^{3+} replacement of Fe^{3+} in the spinel lattice produced desirable modifications to the cobalt ferrite microstructure and characteristics.

Acknowledgments

This work was supported by the National Natural Science Foundation of China (Grant 51174083).

References

[1] N.G. Busnardo, R.F. Paulino, J.C. Afonso, Recovery of cobalt and lithium from spent Li-ion batteries, Quim. Nova. 30 (2007) 995–1000.
[2] T. Georgi-Maschler, B. Friedrich, R. Weyhe, H. Heegn, M. Rutz, Development of a recycling process for Li-ion batteries, J. Power Sources 207 (2012) 173–182.
[3] Y. Huang, G. Han, J. Liu, W. Chai, W. Wang, S. Yang, S. Su, A stepwise recovery of metals from hybrid cathodes of spent Li-ion batteries with leaching-flotation-precipitation process, J. Power Sources 325 (2016) 555–564.
[4] Y.J. Yu, X. Wang, D. Wang, K. Huang, L.J. Wang, L.Y. Bao, F. Wu, Environmental characteristics comparison of Li-ion batteries and Ni-MH batteries under the uncertainty of cycle performance, J. Hazard Mater. 229 (2012) 455–460.
[5] L. Yao, Y. Feng, G. Xi, A new method for the synthesis of $LiNi_{1/3}Co_{1/3}Mn_{1/3}O_2$ from waste lithium ion batteries, RSC Adv. 5 (2015) 44107–44114.
[6] L. Yao, H.S. Yao, G.X. Xi, Y. Feng, Recycling and synthesis of $LiNi_{1/3}Co_{1/3}Mn_{1/3}O_2$ from waste lithium ion batteries using D,L-malic acid, RSC Adv. 6 (2016) 17947–17954.
[7] L. Yaug, G. Xi, Y. Xi, Recovery of Co, Mn, Ni, and Li from spent lithium ion batteries for the preparation of $LiNi_xCo_yMn_zO_2$ cathode materials, Ceram. Int. 41 (2015) 11498–11503.
[8] S.D. Bhame, P.A. Joy, Enhanced magnetostrictive properties of $CoFe_2O_4$ synthesized by an autocombustion method, Sensor. Actuat. A-Phys. 137 (2007) 256–261.
[9] K.K. Mohaideen, P.A. Joy, Studies on the effect of sintering conditions on the magnetostriction characteristics of cobalt ferrite derived from nanocrystalline powders, J. Eur. Ceram. Soc. 34 (2014) 677–686.
[10] I.C. Nlebedim, N. Ranvah, P.I. Williams, Y. Melikhov, J.E. Snyder, A.J. Moses, D.C. Jiles, Effect of heat treatment on the magnetic and magnetoelastic properties of cobalt ferrite, J. Magn. Magn. Mater. 322 (2010) 1929–1933.
[11] I.C. Nlebedim, N. Ranvah, P.I. Williams, Y. Melikhov, F. Anayi, J.E. Snyder, A.J. Moses, D.C. Jiles, Influence of vacuum sintering on microstructure and magnetic properties of magnetostrictive cobalt ferrite, J. Magn. Magn. Mater. 321 (2009) 2528–2532.
[12] K.K. Mohaideen, P.A. Joy, High magnetostriction coefficient of Mn substituted cobalt ferrite sintered from nanocrystalline powders and after magnetic field annealing, Curr. Appl. Phys. 13 (2013) 1697–1701.
[13] P.A.J.P.N. Anantharamaiah, High magnetostriction parameters of sintered and magnetic field annealed Ga-substituted $CoFe_2O_4$, Mater. Lett. 192 (2016) 169–172.
[14] P.N. Anantharamaiah, P.A. Joy, Magnetic and magnetostrictive properties of aluminium substituted cobalt ferrite synthesized by citrate-gel method, J. Mater. Sci. 50 (2015) 6510–6517.
[15] V.L. Mathe, A.D. Sheikh, Magnetostrictive properties of nanocrystalline Co-Ni ferrites, Physica. B. 405 (2010) 3594–3598.
[16] A.M. Pachpinde, M.M. Langade, K.S. Lohar, S.M. Patange, Sagar E. Shirsath, Impact of larger rare earth Pr^{3+} ions on the physical properties of chemically derived $Pr_xCoFe_{2-x}O_4$ nanoparticles, Chem. Phys. 429 (2014) 20–26.
[17] G. Bulai, L. Diamandescu, I. Dumitru, S. Gurlui, M. Feder, O.F. Caltun, Effect of rare earth substitution in cobalt ferrite bulk materials, J. Magn. Magn. Mater. 390 (2015) 123–131.
[18] G. Xi, L. Wang, T. Zhao, Magnetic and magnetostrictive properties of RE-doped Cu-Co ferrite fabricated from spent lithium-ion batteries, J. Magn. Magn. Mater. 424 (2017) 130–136.
[19] G.X. Xi, Y.B. Xi, Effects on magnetic properties of different metal ions substitution cobalt ferrites synthesis by sol-gel auto-combustion route using used batteries, Mater. Lett. 164 (2016) 444–448.
[20] L. Yao, Y.B. Xi, G.X. Xi, Y. Feng, Synthesis of cobalt ferrite with enhanced magnetostriction properties by the sol-gel-hydrothermal route using spent Li-ion battery, J. Alloy. Compd. 680 (2016) 73–79.
[21] L. Yang, G. Xi, T. Lou, X. Wang, J. Wang, Y. He, Preparation and magnetic performance of $Co_{0.8}Fe_{2.2}O_4$ by a sol-gel method using cathode materials of spent Li-ion batteries, Ceram. Int. 42 (2016) 1897–1902.
[22] R.S. Yadav, J. Havlica, I. Kuritka, Z. Kozakova, J. Masilko, M. Hajduchova, V. Enev, J. Wasserbauer, Effect of Pr^{3+} substitution on structural and magnetic properties of $CoFe_2O_4$ spinel ferrite nanoparticles, J. Supercond. Nov. Magn. 28 (2015) 241–248.
[23] M.T. Farid, I. Ahmad, S. Aman, M. Kanwal, G. Murtaza, I. Ali, I. Ahmad, M. Ishfaq, Structural, electrical and dielectric behavior of $Ni_xCo_{1-x}Nd_yFe_{2-y}O_4$ nano-ferrites synthesized by sol-gel method, Dig. J. Nanomater. Bios. 10 (2015) 265–275.
[24] K.S. Lohar, A.M. Pachpinde, M.M. Langade, R.H. Kadam, S.E. Shirsath, Self-propagating high temperature synthesis, structural morphology and magnetic interactions in rare earth Ho^{3+} doped $CoFe_2O_4$ nanoparticles, J. Alloy. Compd. 604 (2014) 204–210.
[25] L. Zhao, H. Yang, X. Zhao, L. Yu, Y. Cui, S. Feng, Magnetic properties of $CoFe_2O_4$ ferrite doped with rare earth ion, Mater. Lett. 60 (2006) 1–6.

[26] G.S.N. Rao, O.F. Caltun, K.H. Rao, P. Rao, B.P. Rao, Improved magnetostrictive properties of Co-Mn ferrites for automobile torque sensor applications, J. Magn. Magn. Mater. 341 (2013) 60–64.
[27] I.C. Nlebedim, M. Vinitha, P.J. Praveen, D. Das, D.C. Jiles, Temperature dependence of the structural, magnetic, and magnetostrictive properties of zinc-substituted cobalt ferrite, J. Appl. Phys. 113 (2013), 193904.
[28] P.N. Anantharamaiah, P.A. Joy, Enhancing the strain sensitivity of $CoFe_2O_4$ at low magnetic fields without affecting the magnetostriction coefficient by substitution of small amounts of Mg for Fe, Phys. Chem. Chem. Phys. 18 (2016) 10516–10527.
[29] K.K. Mohaideen, P.A. Joy, High magnetostriction parameters for low-temperature sintered cobalt ferrite obtained by two-stage sintering, J. Magn. Magn. Mater. 371 (2014) 121–129.